

Coherent Development of Neutrino Flavor in the Supernova Environment

Huaiyu Duan and George M. Fuller

Department of Physics, University of California, San Diego, La Jolla, CA 92093-0319

J. Carlson

Theoretical Division, Los Alamos National Laboratory, Los Alamos, NM 87545

Yong-Zhong Qian

School of Physics and Astronomy, University of Minnesota, Minneapolis, MN 55455

(Dated: February 7, 2020)

We calculate coherent neutrino and antineutrino flavor transformation in the supernova environment, for the first time including a self-consistent treatment of forward scattering-induced coupling and entanglement of intersecting neutrino/antineutrino trajectories. For neutrino mass-squared difference $|\delta m^2| = 3 \times 10^{-3} \text{ eV}^2$ we find that in the normal (inverted) mass hierarchy the more tangentially-propagating (radially-propagating) neutrinos and antineutrinos can initiate collective, simultaneous medium-enhanced flavor conversion of these particles across broad ranges of energy and propagation direction. Accompanying alterations in neutrino/antineutrino energy spectra and/or fluxes could affect supernova nucleosynthesis and the expected neutrino signal.

PACS numbers: 14.60.Pq, 97.60.Bw

In this letter we present the first self-consistent solution to a long standing problem in following coherent flavor inter-conversion among neutrinos and antineutrinos in the region above the hot proto-neutron star subsequent to the supernova explosion [1]. The problem is that flavor histories on intersecting neutrino/antineutrino world lines can be coupled by neutral-current forward exchange scattering [2]. Many studies neglecting this aspect of flavor transformation [2, 3, 4, 5, 6, 7, 8, 9, 10] nevertheless have shown that flavor conversion in the neutrino and antineutrino fields above the proto-neutron star could be important in understanding the supernova explosion mechanism [3, 4, 5] and the origin of heavy *r*-process nuclei [2, 6, 7, 8, 9, 10].

Inelastic scattering processes and associated decoherence may dominate neutrino flavor development in the proto-neutron star core and in the region near the neutrino sphere, necessitating a full quantum kinetic approach there [11, 12]. By contrast, in the hot bubble (a high-entropy region that develops above the neutrino sphere at time post-core-bounce $t_{\text{PB}} \gtrsim 3 \text{ s}$), where the

r-process elements may be made, neutrinos and antineutrinos for the most part propagate coherently. In this limit we can model the evolution of flavor along a *single* neutrino's trajectory with a mean field [13], Schrödinger-like equation, which in the effective 2×2 mixing channel is

$$i \frac{d}{dt} \begin{pmatrix} a_{e\alpha} \\ a_{\tau\alpha} \end{pmatrix} = \hat{H}_f \begin{pmatrix} a_{e\alpha} \\ a_{\tau\alpha} \end{pmatrix}. \quad (1)$$

The effective neutrino flavor evolution Hamiltonian can be expressed in the flavor basis as

$$\hat{H}_f = \begin{pmatrix} -\Delta \cos 2\theta + A + B & \Delta \sin 2\theta + B_{e\tau} \\ \Delta \sin 2\theta + B_{e\tau}^* & \Delta \cos 2\theta - A - B \end{pmatrix}. \quad (2)$$

The flavor evolution of an antineutrino is determined similarly but with $A \rightarrow -A$, $B \rightarrow -B$ and $B_{e\tau} \rightarrow -B_{e\tau}^*$. In these expressions t is an Affine parameter along the neutrino's world line, $\Delta \equiv \delta m^2/2E_\nu$, where E_ν is neutrino energy, and δm^2 is the difference of the squares of the vacuum neutrino mass eigenvalues. To represent the measured atmospheric neutrino scale, we set $\delta m^2 = \pm 3 \times 10^{-3} \text{ eV}^2$, where the plus (minus) sign is for the normal (inverted) mass hierarchy. In Eq. (2), θ is the effective 2×2 vacuum mixing angle, which will be $\sim \theta_{13}$. Current experimental bounds give $\sin^2 2\theta_{13} \lesssim 0.1$ [14] and in our numerical calculations we use $\theta = 0.1$. The flavor diagonal potentials in Eq. (2) are A , from ν_e -electron forward scattering (determined by the matter density profile in the hot bubble [1]), and B , from neutrino-neutrino forward scattering. The flavor off-diagonal potential $B_{e\tau}$ similarly stems from neutrino-neutrino forward exchange scattering [15]. Eq. (1) is nonlinear in that the potentials B and $B_{e\tau}$ depend on the amplitudes $a_{e\alpha}$ and $a_{\tau\alpha}$ for a neutrino with initial flavor state $\alpha = e, \tau$ to be either elec-

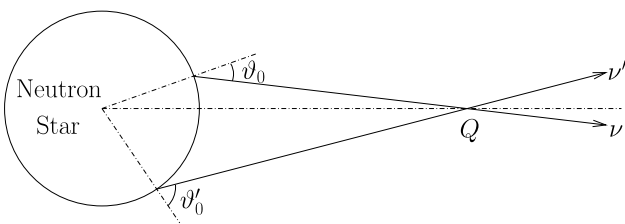


FIG. 1: Flavor evolution of neutrino ν on trajectory designated by angle ϑ_0 relative to the neutron star surface normal is entangled with the flavor development of all neutrinos ν' on intersecting trajectories.

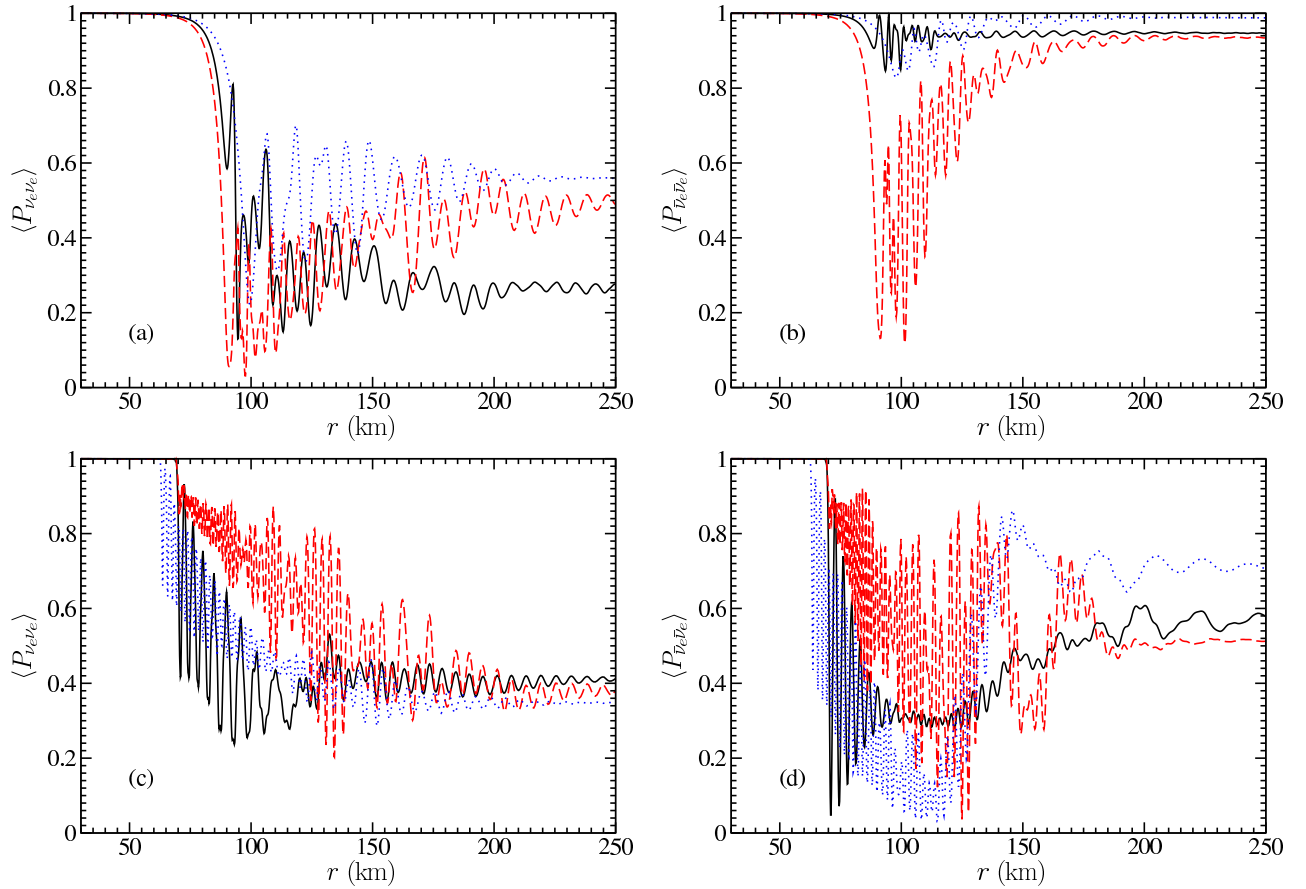


FIG. 2: (Color online) Plots of energy-averaged survival probabilities $\langle P_{\nu\nu} \rangle$ for ν_e (left panels) and $\bar{\nu}_e$ (right panels) as functions of radius r for the normal (upper panels) and inverted (lower panels) neutrino mass hierarchies, respectively. The solid and dashed lines give average survival probabilities along the trajectories $\cos \vartheta_0 = 1$ and $\cos \vartheta_0 = 0$, respectively, as computed in the multi-angle simulations. The dotted lines give the average survival probabilities computed in the single-angle simulations.

tron or tau flavor, respectively. However, the true complexity of this problem arises from quantum mechanical and geometrical entanglement of neutrino/antineutrino flavor histories as illustrated in Fig. 1: B and $B_{e\tau}$ help determine the flavor development at point Q on neutrino ν 's world line, but these potentials depend on a coherent sum over all neutrinos ν' passing through Q . Here ν_τ designates the relevant combination of mu and tau flavor neutrinos assuming these species are maximally mixed in vacuum and in the supernova medium [16]. In our example numerical calculations we have taken the initial neutrino and antineutrino energy spectra to be of Fermi-Dirac form, with degeneracy parameter $\eta_\nu = 3$ and average energies $\langle E_{\nu_e} \rangle = 11$ MeV, $\langle E_{\bar{\nu}_e} \rangle = 16$ MeV, and $\langle E_{\nu_\tau, \bar{\nu}_\tau} \rangle = 25$ MeV and we take the energy luminosity for each neutrino species to be $L_\nu = 10^{51}$ erg s $^{-1}$.

Though neutrinos and antineutrinos are emitted from the neutrino sphere (radius $r = 11$ km) in a thermal, incoherent manner, our simulations show that large scale coherence and collective flavor transformation develops with increasing radius r . This behavior is driven in part

by progressive forward scattering-induced entanglement of flavor evolution on intersecting neutrino and antineutrino world lines. Near the neutron star surface, where electrons are degenerate, $A \gg B$, $B_{e\tau} \approx 0$, and ordinary Mikheyev-Smirnov-Wolfenstein (MSW) [17, 18, 19] flavor evolution obtains. However, at larger r , B and $B_{e\tau}$ can dominate and flavor evolution can be very different from MSW. For the normal mass hierarchy, our simulations show that the more tangentially-propagating neutrinos and antineutrinos, which experience the largest B and $B_{e\tau}$ potentials because of the intersection angle dependence in the weak current [2, 3], are the first to experience significant flavor transformation for a broad range of energies. This sets in, *e.g.*, at $r \approx 80$ km if the entropy-per-baryon in the hot bubble is $S = 140$ in units of Boltzmann's constant k_B . This simultaneous conversion of ν_α and $\bar{\nu}_\alpha$ quickly spreads to all neutrino/antineutrino trajectories, leading to coherent, collective flavor oscillations of the entire neutrino/antineutrino field. In the inverted mass hierarchy, the opposite is true: radially-propagating neutrinos and antineutrinos transform first.

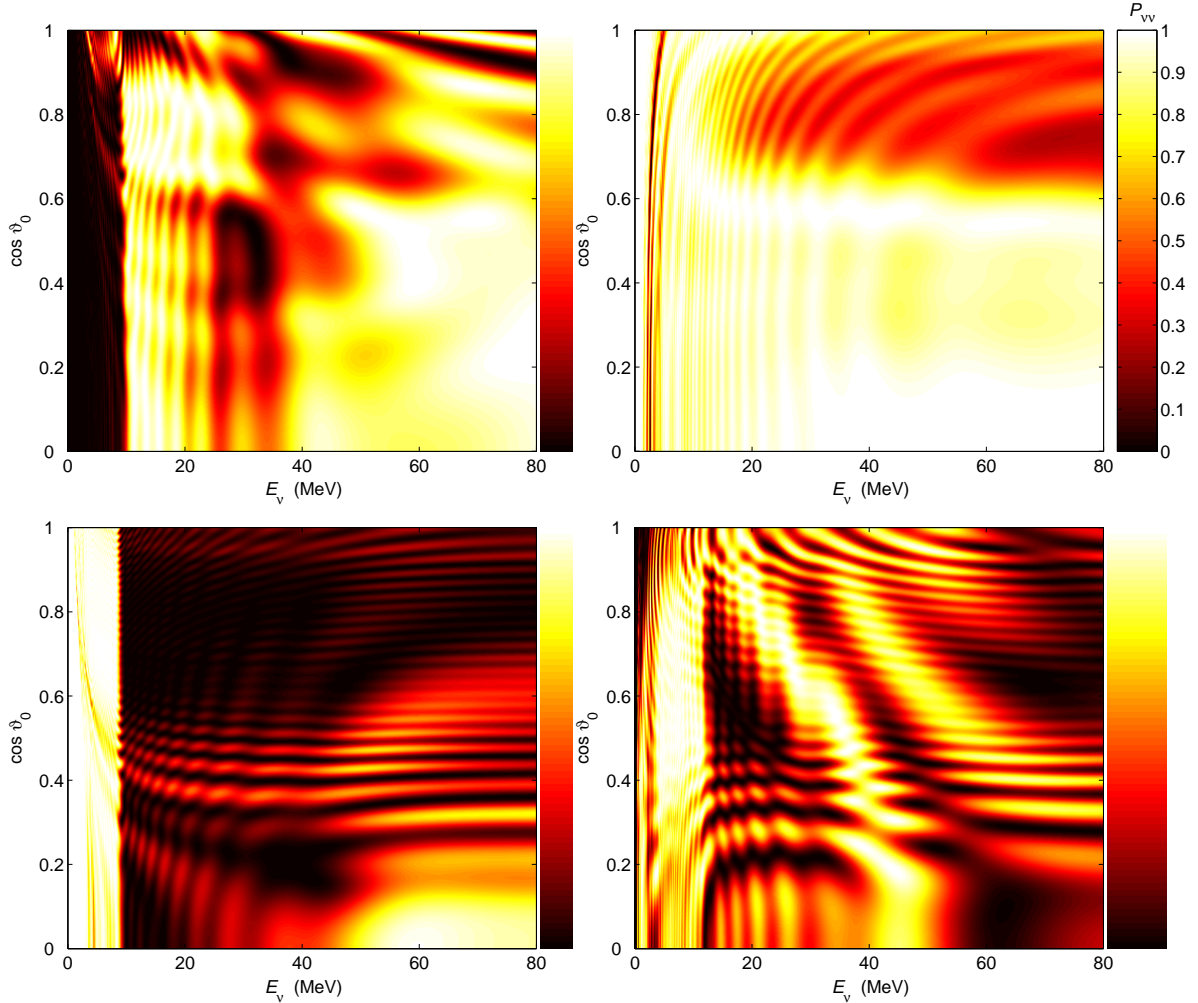


FIG. 3: (Color online) Plots of survival probabilities $P_{\nu\nu}$ for neutrinos (left panels) and antineutrinos (right panels) as functions of both neutrino energy E_{ν} and emission angle ϑ_0 at radius $r = 250$ km. The upper panels employ a normal neutrino mass hierarchy, and the lower panels employ an inverted neutrino mass hierarchy.

These features of flavor development can be seen in Fig. 2. The survival probability at location t along a given neutrino's world line is, *e.g.*, for a neutrino which is initially electron flavor, $P_{\nu_e \nu_e}(t, \vartheta_0, E_{\nu}) = |a_{ee}(t)|^2$. In Fig. 2 we show the energy-spectrum-averaged survival probabilities $\langle P_{\nu\nu} \rangle$ for ν_e and $\bar{\nu}_e$ as functions of r for both the normal and the inverted neutrino mass hierarchy cases. It is clear that flavor evolution along different trajectories can be different, yet it is also evident that neutrinos and antineutrinos can undergo simultaneous, significant medium-enhanced flavor conversion. Our simulations show that this conversion can take place over broad ranges of neutrino and antineutrino energy. We have also performed simulations using the single-angle approximation widely adopted in the literature. These give results *qualitatively* similar to our multi-angle calculations, as shown in Fig. 2. The collective neutrino flavor transformation observed in our simulations is not the

“synchronized” mode described in Ref. [7]. In the normal mass hierarchy case, neutrinos or antineutrinos in the synchronized mode undergo one-time transformation in the same way as does a neutrino with energy p_{sync} [7]. There would be little synchronized flavor transformation in the inverted neutrino mass hierarchy.

The collective neutrino flavor transformation evident in Fig. 2 is likely of the “bi-polar” type as described in Ref. [20]. In this mode, neutrinos and antineutrinos experience in-phase, collective, semi-periodic flavor oscillations, even for the inverted mass hierarchy. This behavior was first observed in numerical simulations of neutrino flavor transformation in the early universe [21, 22]. It has been argued [20] that neutrinos and antineutrinos could undergo collective flavor transformation in the bi-polar mode for the inverted mass hierarchy case even in the presence of a dominant matter potential. This conjecture seems to be supported by our simulations.

Using the single-angle approximation, we have studied the relation between r_X , the radius where large-scale flavor transformation first occurs, and the entropy per baryon S and neutrino luminosity L_ν . With larger S the matter density profile is more condensed toward the neutrino sphere. We find that, for the normal neutrino mass hierarchy case, r_X decreases substantially if S is increased from 140 to 250. However, the value of r_X decreases only slightly with the same change in S for the inverted neutrino mass hierarchy case. The non-linear effect of the neutrino-neutrino forward scattering potentials is enhanced with higher L_ν . For the normal neutrino mass hierarchy case, r_X decreases monotonically with increasing L_ν , and approaches the radius where neutrinos and antineutrinos start collective flavor transformation in the synchronized mode. In the inverted neutrino mass hierarchy, r_X increases monotonically with increasing L_ν .

In Fig. 3 we show survival probabilities $P_{\nu\nu}$ as functions of both neutrino energy E_ν and emission angle ϑ_0 at radius $r = 250$ km. Large-scale quantum interference stemming from entanglement of flavor histories is evident. The horizontal “fringes” in Fig. 3 are generated during neutrino/antineutrino background-dominated collective flavor transformation. In this regime E_ν is unimportant, but ϑ_0 is crucial. This is because the neutrino-neutrino forward scattering potentials are energy-blind but have a strong angle dependence. The vertical “fringes” are generated at larger r where the neutrino background is weaker and, therefore, (non-adiabatic) MSW transformation dominates flavor evolution. In this case ϑ_0 is unimportant and E_ν is crucial. This is because at large r the neutrino beams are almost parallel to each other, and the MSW effect is energy dependent. Our simulations show sharp, vertical transition regions at $E_\nu \simeq 10$ MeV for neutrinos in both the normal and inverted neutrino mass hierarchies. This feature is likely a result of break-down of collective transformation [1].

The neutron-to-proton ratio n/p in the hot bubble is set largely at $r \lesssim 100$ km for $S \sim 100$ by a competition between $\nu_e + n \rightarrow p + e^-$ and $\bar{\nu}_e + p \rightarrow n + e^+$ [6]. Our calculations show that in this radius regime collective flavor transformation could engineer significant alteration of the ν_e and $\bar{\nu}_e$ energy spectra. This could result in an alteration in n/p which could affect the prospects for r -process nucleosynthesis. In broad brush, across all ϑ_0 mostly lower energy ν_e and few $\bar{\nu}_e$ are transformed in the normal mass hierarchy. The opposite is true in the inverted mass hierarchy. However, as is evident in Fig. 3 at $r = 250$ km, in either mass hierarchy, survival probability can show significant ϑ_0 dependence. The ν_e and $\bar{\nu}_e$ energy spectra and angular distributions could be quite different from those in zero-neutrino-mass supernova models, with possibly important effects on nucle-

osynthesis and the expected neutrino signal.

This work was supported in part by a UC/LANL CARE grant, NSF grant PHY-04-00359, the Terascale Supernova Initiative (TSI) collaboration’s DOE SciDAC grant at UCSD, DOE grant DE-FG02-87ER40328 at UMN, and by the LDRD Program and Open Supercomputing at LANL. We would like to thank A. B. Balantekin, S. Bruenn, C. Y. Cardall, J. Hayes, W. Landry, O. E. B. Messer, A. Mezzacappa, M. Patel, G. Raffelt and H. Yüksel for valuable conversations.

- [1] H. Duan, G. M. Fuller, J. Carlson, and Y.-Z. Qian (2006), astro-ph/0606616.
- [2] Y. Z. Qian and G. M. Fuller, Phys. Rev. **D51**, 1479 (1995), astro-ph/9406073.
- [3] G. M. Fuller, R. W. Mayle, J. R. Wilson, and D. N. Schramm, Astrophys. J. **322**, 795 (1987).
- [4] G. M. Fuller, R. W. Mayle, B. S. Meyer, and J. R. Wilson, Astrophys. J. **389**, 517 (1992).
- [5] A. Mezzacappa and S. Bruenn, in *Proceeding of the Second International Workshop on the Identification of Dark Matter*, edited by N. J. C. Spooner and V. Kudryavtsev (World Scientific, Singapore, 1999).
- [6] Y.-Z. Qian, G. M. Fuller, G. J. Mathews, R. W. Mayle, J. R. Wilson, and S. E. Woosley, Phys. Rev. Lett. **71**, 1965 (1993).
- [7] S. Pastor and G. Raffelt, Phys. Rev. Lett. **89**, 191101 (2002), astro-ph/0207281.
- [8] Y.-Z. Qian and G. M. Fuller, Phys. Rev. **D52**, 656 (1995), astro-ph/9502080.
- [9] A. B. Balantekin and H. Yüksel, New J. Phys. **7**, 51 (2005), astro-ph/0411159.
- [10] G. M. Fuller and Y.-Z. Qian, Phys. Rev. **D73**, 023004 (2006), astro-ph/0505240.
- [11] G. Sigl and G. Raffelt, Nucl. Phys. **B406**, 423 (1993).
- [12] P. Strack and A. Burrows, Phys. Rev. **D71**, 093004 (2005), hep-ph/0504035.
- [13] A. Friedland and C. Lunardini, JHEP **10**, 043 (2003), hep-ph/0307140.
- [14] G. L. Fogli, E. Lisi, A. Marrone, and A. Palazzo, Prog. Part. Nucl. Phys. **57**, 742 (2006), hep-ph/0506083.
- [15] J. T. Pantaleone, Phys. Rev. **D46**, 510 (1992).
- [16] A. B. Balantekin and G. M. Fuller, Phys. Lett. **B471**, 195 (1999), hep-ph/9908465.
- [17] L. Wolfenstein, Phys. Rev. **D17**, 2369 (1978).
- [18] L. Wolfenstein, Phys. Rev. **D20**, 2634 (1979).
- [19] S. P. Mikheyev and A. Y. Smirnov, Yad. Fiz. **42**, 1441 (1985).
- [20] H. Duan, G. M. Fuller, and Y.-Z. Qian (2005), astro-ph/0511275.
- [21] V. A. Kostelecky and S. Samuel, Phys. Lett. **B318**, 127 (1993).
- [22] V. A. Kostelecky and S. Samuel, Phys. Lett. **B385**, 159 (1996), hep-ph/9610399.